Theoretical Investigations of the Reactivities of Cationic Six-membered Carbene Analogues of Group 14 Elements

Ren-Hong Wang and Ming-Der Su*

Department of Applied Chemistry, National Chiayi University, Chiayi 60004, Taiwan

Received: March 27, 2008; Revised Manuscript Received: June 13, 2008

The potential energy surfaces for the chemical reactions of cationic six-membered group 14 heavy carbene species have been studied using density functional theory (B3LYP/LANL2DZ) and CCSD (CCSD/LANL2DZ//B3LYP/LANL2DZ) methods. Five six-membered group 14 cationic heavy carbene species, $[HC(CMeNPh)_2E:]^+$, where E = C, Si, Ge, Sn, and Pb, have been chosen as model reactants in this work. Also, four kinds of chemical reaction, C−H bond insertion, multiple bond cycloaddition, dimerization, and O−H bond insertion, have been used to study the chemical reactivities of these group 14 cationic carbene species. Basically, our present theoretical work predicts that the larger the ∠NEN bond angle and the smaller the singlet−triplet splitting of the carbene, the lower its activation barriers will be and, in turn, the more rapid are its chemical reactions with other species. Moreover, the theoretical investigations suggest that the relative carbenic reactivity decreases in the order C > Si > Ge > Sn > Pb. That is, the heavier the group 14 atom (E), the more stable is its cationic carbene toward chemical reaction. As a result, we predict that the cationic six-membered group 14 carbene species (E = C, Si, Ge, Sn, and Pb) should be stable, readily synthesized, and isolated at room temperature. Our computational results are in good agreement with the available experimental observations. Furthermore, the singlet−triplet energy splitting of the carbene, as described in the configuration mixing model attributed to the work of Pross and Shaik, can be used as a diagnostic tool to predict its reactivities. The results obtained allow a number of predictions to be made.

I. Introduction

During the last three decades, the development of the chemistry of divalent group 14 compounds has received wide interest because of their unusual structures and properties[1] when compared with compounds containing the hydride species, such as methylene (H_2C:) and silylene (H_2Si:). Most can be stabilized kinetically by sterically demanding ligands and/or thermodynamically by inter- and intramolecular coordination. Indeed, many nitrogen-containing bulky ligands have been used to stabilize these compounds.[2] Of these, the syntheses of stable cationic carbene-like compounds containing heavy group 14 elements have been a particular challenge to synthetic chemists.

Through the elegant studies performed by Driess and coworkers, kinetically stabilized molecules bearing a cationic six-membered ring, have been synthesized and fully characterized.[3] That is, the kinetic stabilization of the low-coordinate, divalent silicon and germanium center in such molecules can be achieved by favorable N-coordination and planar aromatic six π-electron delocalization. See Scheme 1. Nevertheless, attempts to isolate other cationic analogues—carbene, stannylene, and plumbylene—have all been unsuccessful up to now. Although there have been a few reports concerning the chemical and physical properties of available group 14 cationic heavy carbene species,[4] to the best of our knowledge, neither experimental nor theoretical work has been devoted to a systematic study of their reactivities.

It is these unsolved problems that inspired this study. To elucidate the mechanisms and barrier heights for the group 14 reactivities, we have now undertaken a systematic investigation of the potential energy surfaces of several different kinds of cationic carbene reactions. Three kinds of chemical reactions

SCHEME 1

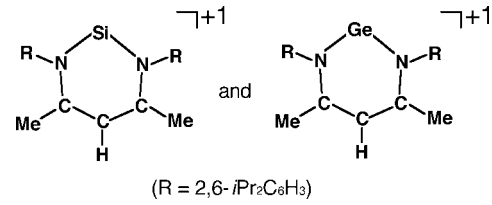

are discussed in the present work. They are insertion, cycloaddition, and dimerization. We therefore present a density functional theory (DFT) study to investigate the potential energy surfaces and mechanisms of the following reactions:

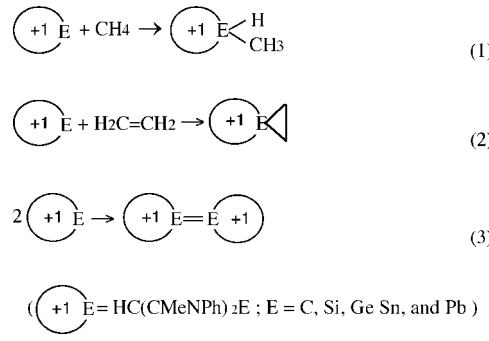

That is, we theoretically consider the reaction paths of three kinds of model reactions involving a series of group 14 cationic heavy carbenes of the type $[HC(CMeNPh)_2E:]^+$, where E = C, Si, Ge, Sn, and Pb. Each of these pathways was examined computationally, and each is described in detail below.

* Corresponding author e-mail: midesu@mail.ncyu.edu.tw.

10.1021/jp8026397 CCC: $40.75
Published on Web 07/25/2008

TABLE 1: Selected Geometric Values and Relative Energies for Singlet and Triplet Group 14 Carbenes, $HC(CMeNPh)_2E$, Where E = C, Si, Ge, Sn, and Pb[a,b]

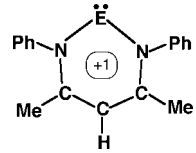

system	E = C	E = Si[c]	E = Ge[d]	E = Sn	E = Pb
			Singlet		
E−N (Å)	1.402	1.823 [1.768]	1.923 [1.865]	2.090	2.164
N−C (Å)	1.383	1.374 [1.365]	1.370 [1.402]	1.369	1.367
C−C (Å)	1.403	1.408 [1.384]	1.409 [1.397]	1.412	1.414
∠NEN (°)	121.0	95.16 [96.50]	92.36 [95.84]	87.78	86.15
			Triplet		
E-N (Å)	1.417	1.838	1.940	2.309	2.401
N−C (Å)	1.367	1.362	1.417	1.333	1.331
C−C (Å)	1.419	1.425	1.422	1.446	1.447
∠NEN (°)	123.1	98.41	93.75	83.05	81.24
ΔE_{st}[e] (kcal mol^{-1})	46.19	59.97	67.28	71.93	77.75

[a] All were calculated at the B3LYP/LANL2DZ (singlet) and UB3LYP/LANL2DZ (triplet) levels of theory. [b] The parameters from experiments are given in brackets. [c] See ref 3a. [d] See ref 3b. [e] Energy relative to the corresponding singlet state. A positive value means the singlet is the ground-state.

Our specific aims are to gain a deeper understanding of the reaction mechanism using the DFT method, to explain trends in the reactivity on varying the element E, and to bring out factors that control the magnitude of the activation barrier. Moreover, a better understanding of the thermodynamic and kinetic aspects of such cationic carbene reactions may shed some light on the optimal design of further related catalytic processes and chemical synthesis.

II. Theoretical Methods

All geometries were fully optimized without imposing any symmetry constraints, although several optimized structures showed various elements of symmetry. For our DFT calculations, we used the hybrid gradient-corrected exchange functional proposed by Becke,[5] combined with the gradient-corrected correlation functional of Lee, Yang, and Parr.[6] Thus, the geometries of all the stationary points were fully optimized at the B3LYP level of theory. These B3LYP calculations were carried out with pseudorelativistic effective core potentials on the group 14 elements modeled using the double-ζ (DZ) basis sets.[7] Accordingly, we denote our B3LYP calculations by B3LYP/LANL2DZ. It is noted that the model compounds $HC(CMeNPh)_2E$ have 213 (136 electrons) basis functions for E = C, Si, Ge, Sn, and Pb. The spin-unrestricted (UB3LYP) formalism was used for the open-shell (triplet) species. The computed expectation values of the spin-squared operator $<S^2>$ were in the range of 2.001−2.023 for the triplet species considered here. Therefore, they were very close to the correct value of 2.0 for pure triplets, so that their geometries and energetics are reliable for this study.

Frequency calculations were performed on all structures to confirm that the reactants and products had no imaginary frequencies and that transition states (TSs) possessed only one imaginary frequency. The relative energies at 0 K were thus corrected for vibrational zero-point energies (ZPE, not scaled). Thermodynamic corrections to 298 K, ZPE corrections, heat capacity corrections, and entropy corrections (ΔS) obtained were applied at the B3LYP/LANL2DZ level. Thus, the relative free energy (ΔG) at 298 K was also calculated at the same level of theory. For better energetics, single-point energies were also calculated at CCSD(FC)/LANL2DZ//B3LYP/LANL2DZ + ZPE (B3LYP/ LANL2DZ) (or CCSD),[8] to improve the treatment of electron correlation. All of the DFT calculations were performed using the GAUSSIAN 03 package of programs.[9]

III. Results and Discussion

1. Geometries and Electronic Structures of $[HC(CMeNPh)_2E:]^+$. Before discussing the geometrical optimizations and the potential energy surfaces for the chemical reactions of the cationic heavy carbene species, we shall first examine the geometries and electronic structures of the reactants, that is, $[HC(CMeNPh)_2E:]^+$ (E = C, Si, Ge, Sn, and Pb). The optimized geometries for these four valence-electron carbenic cations were calculated at the B3LYP/LANL2DZ level of theory, and their selected geometrical parameters are collected in Table 1, where they are compared with some available experimental data.[3] The relative energies obtained from DFT calculations are also summarized in Table 1. Their Cartesian coordinates are included in the Supporting Information.

In the present work, reactants $[HC(CMeNPh)_2E:]^+$ (E = C, Si, Ge, Sn, and Pb) have been calculated both as singlet and as triplet species, whose geometric parameters are shown in Table 1. As mentioned earlier, although only two crystallographic investigations on substituted $[HC(CMeNPh)_2Si:]^+$ and $[HC(CMeNPh)_2Ge:]^+$ have been carried out during the last two years, no theoretical calculations are so far available in the literature for these compounds. Our B3LYP calculations predict that the average Si−N and Ge−N bond lengths in the singlet state are 1.823 and 1.923 Å, which can be compared with the experimental values 1.768 and 1.865 Å,[3] respectively. The greater bond lengths at silicon and germanium are somewhat surprising and are presumably due to the larger size of the aryl substituent at the nitrogens.[3] Similarly, the calculated N−C bond length in $[HC(CMeNPh)_2Si:]^+$ (average 1.374 Å at B3LYP) and $[HC(CMeNPh)_2Ge:]^+$ (average 1.370 Å at B3LYP) compare favorably with those determined from X-ray data in $[HC(CMeNPh)_2Si:]^+$ (1.365 Å) and $[HC(CMeNPh)_2Ge:]^+$ (1.402 Å), respectively, reported by Driess et al.[3] On the other hand, the ∠NSiN angle in $[HC(CMeNPh)_2Si:]^+$ and the ∠NGeN angle in $[HC(CMeNPh)_2Ge:]^+$ are 95.16 and 92.36°, respectively, which agree reasonably well with the experimental values (96.50 and 95.84°,[3] respectively) as given in Table 1, bearing in mind that the experimental

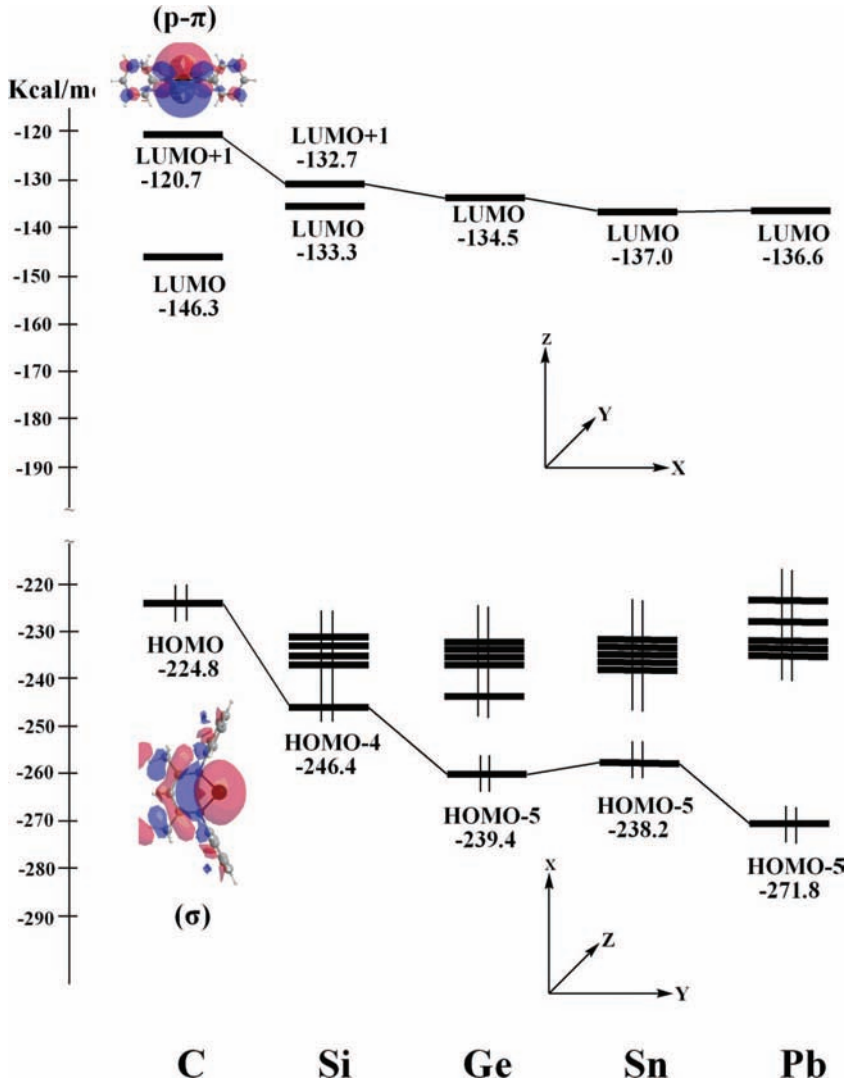

Figure 1. Calculated frontier molecular orbitals for the $[HC(CMeNPh)_2E:]^+$ (E = C, Si, Ge, Sn, and Pb) species. For more information see the text.

structures contain bulkier groups. Namely, the differences may be attributed to steric effects that cause the experimentally studied $[HC(CMeNPh)_2Si:]^+$ and $[HC(CMeNPh)_2Ge:]^+$ to have larger ∠NEN bond angles than the species studied theoretically. Basically, as can be seen in Table 1, the agreement for both bond lengths and bond angles in the rings (E = Si and Ge) between the B3LYP results and experiments[3] for the singlet state is quite good, with the bond lengths and angles in agreement to within 0.058Å and 3.5°, respectively. As a result of this encouraging agreement, it is believed that the B3LYP calculations will provide an adequate theoretical level for further investigations of the molecular geometries, electronic structures, and kinetic features of the reactions.

As expected, irrespective of the multiplicity of the group 14 cationic heavy carbene, our computations suggest that the E−N bond distance increases monotonically down the group from C to Pb. The reason for this is mainly due to the increase in atomic radius of E from carbon to lead. As can be seen in Table 1, the singlet ∠NEN bond angles at the C, Si, Ge, Sn, and Pb centers in the $[HC(CMeNPh)_2E:]^+$ species, decreases in the order 123° (C) > 95.2° (Si) > 92.4° (Ge) > 87.8° (Sn) > 86.2° (Pb). Likewise, the triplet ∠NEN bond angles follow the same trend: 119° (C) > 98.4° (Si) > 93.8° (Ge) > 83.1 (Sn) > 81.2° (Pb). Besides this, it is apparent that as the E atom becomes heavier a more acute ∠NEN bond angle is favored in both singlet and triplet $[HC(CMeNPh)_2E:]^+$. The reason for this may be due to the "orbital nonhybridization effect", also known as the "inert s-pair effect".[10] As is well-known, tin (as well as lead) has a low tendency to form hybrid orbitals with high p character because of the size difference between the valence s and p atomic orbitals.[10] Accordingly, the carbenic center (E) tends to form a nonbonding orbital acquiring mainly s-characters, whereas the remaining p-electrons are used up to form π bonds with the neighboring nitrogen atoms. Consequently, the valence s and p orbitals of the heavier members of the group overlap less to form strong hybrid orbitals.[10] It is therefore expected that a $[HC(CMeNPh)_2E:]^+$ compound with a heavier E center favors a smaller bond angle ∠NEN.

In the case of cyclic $[HC(CMeNPh)_2E:]^+$ (E = C, Si, and Ge) reactants, other interesting trends observed in Table 1 are the increase in the bond distance E−N and in the bond angle ∠NEN on going from the singlet to the triplet state. On the other hand, the triplet state of $[HC(CMeNPh)_2Sn:]^+$ and $[HC(CMeNPh)_2Pb:]^+$ have a significantly greater bond distance (E−N) and a narrow bond angle ∠NEN than their closed shell singlet. The reason for these phenomena can be understood simply by considering their electronic structures (vide infra).

Figure 1 is a molecular orbital correlation diagram of valence orbitals for $[HC(CMeNPh)_2E:]^+$(E = C, Si, Ge, Sn, and Pb). Substitution of a single E atom at the $[HC(CMeNPh)_2E:]^+$ center decreases the energy of the σ orbital on going from C to Pb, that is, E σ(C) > E σ(Si) > E σ(Ge) > E σ(Sn) > E σ(Pb). Likewise, this substitution also decreases the p$-\pi$ orbital energy, that is, E p$-\pi$(C) > E p$-\pi$(Si) > E p$-\pi$(Ge) > E p$-\pi$(Sn) > E p$-\pi$(Pb). Note that the nature of the σ and the p$-\pi$ orbitals in $[HC(CMeNPh)_2E:]^+$ are quite different from those encountered in traditional group 14 divalent compounds.[11] For instance, the HOMO of $[HC(CMeNPh)_2C:]^+$ is essentially a nonbonding σ orbital. This lone pair orbital is arranged in the cyclic plane of the $[HC(CMeNPh)_2E:]^+$ species, in a pseudotrigonal planar fashion with respect to the two sets of E$-$N linkages. As a result, such lone pairs can be viewed as located within an orbital of predominant sp^2-character. It should be noted that the existence of a nonbonded lone pair of electrons at the E center strongly endorses the singlet carbene character of the group 14 divalent molecules (vide infra). Similarly, the vacant p$-\pi$ orbital is situated on the LUMO + 1 energy level of the $[HC(CMeNPh)_2C:]^+$ species as shown in Figure 1. On the other hand, our theoretical findings indicate that the HOMO in the $[HC(CMeNPh)_2E:]^+$ (E = Si, Ge, Sn, and Pb) case is entirely ligand-based and of π symmetry. Besides this, our computations show that, for the $[HC(CMeNPh)_2E:]^+$ (E = Ge, Sn, and Pb) compounds, although their LUMOs correspond to the E p$-\pi$ orbital, their HOMOs do not involve the E lone pair. The latter is the HOMO$-$5 level, and separated from the corresponding LUMO by about 105 (Ge), 101 (Sn), and 135 (Pb) kcal/mol, respectively. The reason for such molecular orbital locations may be attributed to the "orbital non-hybridization effect", also known as the inert s-pair effect, as discussed earlier.[10]

Furthermore, the other striking feature is the singlet$-$triplet splitting ($\Delta E_{st} = E_{triplet} - E_{singlet}$). As one can see in Table 1, our DFT calculations indicate that the singlet$-$triplet splittings for carbon, silicon, germanium, tin, and lead are 46, 60, 67, 72, and 78 kcal/mol, respectively, that is, ΔE_{st} increases in the order C < Si < Ge < Sn < Pb. In other words, the heavier the central group 14 atom (E), the larger the singlet$-$triplet splitting (ΔE_{st}) of $[HC(CMeNPh)_2E:]^+$. Again, as mentioned earlier, the reason for such a difference can be traced directly to electronic factors. From Figure 1, it is apparent that the magnitude of the energy difference between σ and p$-\pi$ for the cyclic $[HC(CMeNPh)_2E:]^+$ systems becomes larger as one proceeds along the series from C to Pb. Accordingly, our theoretical findings indicate that the electronic perturbation effect, where the symmetry of frontier orbitals changes, should play a significant role in determining the energy ordering of the frontier orbitals. This, in turn, can affect the magnitude of the singlet$-$triplet splitting for such cationic cyclic divalent molecules.

In fact, the stabilities of the carbene analogues are determined by the singlet$-$triplet energy separations in $[HC(CMeNPh)_2E:]^+$. If ΔE_{st} is small, then the carbene-type structures will not be stable and will be capable of facile chemical reactions (such as with solvents, etc.). As already stated in Table 1, our theoretical calculations demonstrated that the group 14 $[HC(CMeNPh)_2E:]^+$ species have comparatively large singlet$-$triplet separations (ΔE_{st} > 46 kcal/mol). In consequence, these species should be stable enough to be detected experimentally. The supporting evidence comes from the fact that so far the silicon and germanium carbeneoid species with a six-membered ring (i.e., $[HC(CMeNPh)_2Si:]^+$ and $[HC(CMeNPh)_2Ge:]^+$) have been experimentally identified and separated.[3]

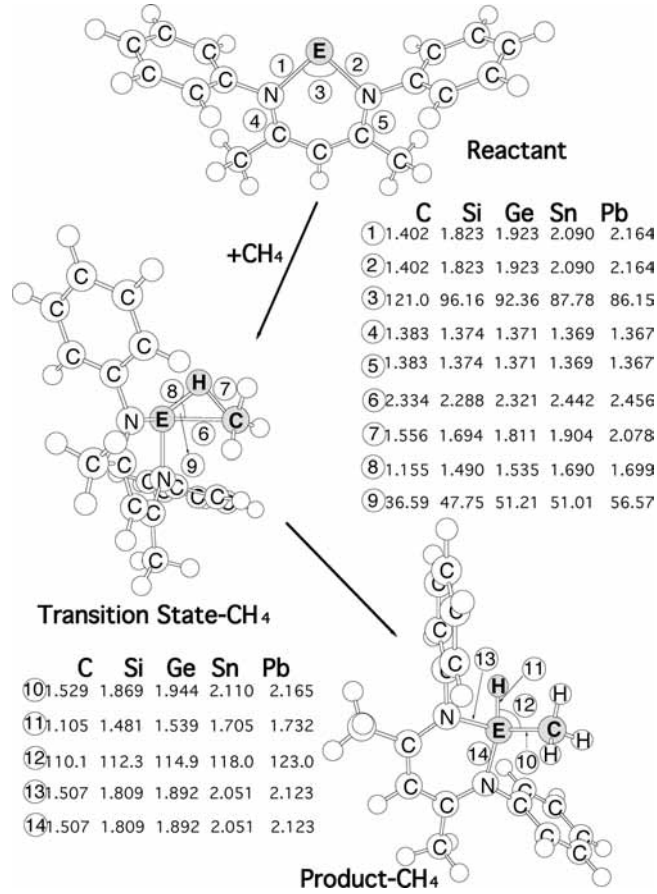

Figure 2. B3LYP/LANL2DZ optimized geometries (in Ångströms and degrees) of the reactants (singlet), transition states, and insertion products of $[HC(CMeNPh)_2E:]^+$ (E = C, Si, Ge, Sn, and Pb) and CH_4. See Table 2 for the relative energies for each species. Hydrogens are omitted for clarity.

Finally, as seen from Table 1, our DFT (and CCSD, vide infra) calculations indicate that the $[HC(CMeNPh)_2E:]^+$ (E = C, Si, Ge, Sn, and Pb) species all possess a singlet ground state. This strongly indicates that all three reactions (eqs 1–3) should proceed on the singlet surface. We shall thus focus on the singlet surface from now on.

2. Geometries and Energetics of $[HC(CMeNPh)_2E:]^+ + CH_4$. We shall now consider mechanisms that proceed via eq 1, focusing on the transition states as well as on the insertion products themselves. That is, the insertion mechanisms may be thought to proceed as follows: reactants (Rea-CH_4) → transition state (TS-CH_4) → products (Pro-CH_4). The optimized geometries calculated at the B3LYP/LANL2DZ level of theory involving Rea-CH_4, TS-CH_4, and Pro-CH_4 are collected in Figure 2. The corresponding relative energies at the B3LYP and CCSD levels of theory are given in Table 2. Cartesian coordinates calculated for the stationary points at the B3LYP level are available as Supporting Information. There are several important conclusions from these results to which attention should be drawn.

Considering the C$-$H bond insertion reaction path, we have located the transition state for each $[HC(CMeNPh)_2E:]^+$ case (TS-$CH_4$$-$C, TS-$CH_4$$-$Si, TS-$CH_4$$-$Ge, TS-$CH_4$$-$Sn, and TS-$CH_4$$-$Pb) at the DFT level of theory. As one can see in Figure 2, all five transition state structures show the same three-center pattern involving E (E = C, Si, Ge, Sn, and Pb), carbon, and hydrogen atoms. The transition state vectors are in accordance with an insertion process, primarily with C$-$H bond stretching accompanied by a hydrogen atom migrating to the E center.

TABLE 2: Relative Energies for Singlet and Triplet Group 14 Cationic Carbene Species ($[HC(CMeNPh)_2E:]^+$) and for the CH_4 Insertion Process: Reactants ($[HC(CMeNPh)_2E:]^+ + CH_4$) → Transition State → Insertion Product[a]

system	ΔE_{st}[b] (kcal mol^{-1})	$\Delta E^{\ddagger}$[c] (kcal mol^{-1})	ΔH[d] (kcal mol^{-1})
E = C	46.19 (46.23)	38.95 (60.08)	−30.21 (−38.96)
E = Si	59.97 (60.39)	66.07 (68.65)	−11.07 (−35.22)
E = Ge	67.28 (70.27)	78.52 (87.45)	7.314 (−7.837)
E = Sn	71.93 (75.77)	88.10 (102.9)	21.50 (12.30)
E = Pb	77.75 (79.96)	109.6 (128.4)	50.40 (46.63)

[a] All were calculated at the B3LYP/LANL2DZ (CCSD results in parentheses) level of theory. For the B3LYP optimized structures of the stationary points, see Figure 2. [b] Energy relative to the corresponding singlet state. A positive value means the singlet is the ground-state. [c] The activation energy of the transition state, relative to the corresponding reactants. [d] The reaction enthalpy of the product, relative to the corresponding reactants.

The B3LYP eigenvalues give imaginary frequencies (cm^{-1}) of 1122*i* (TS-CH_4−C), 1293*i* (TS-CH_4−Si), 1238*i* (TS-CH_4−Ge), 1211*i* (TS-CH_4−Sn), and 1191*i* (TS-CH_4−Pb). As seen in Figure 2, in the transition state, there is a trend as E increases in atomic weight for the stretching C−H bond to become longer, and for the forming E−H bond length to increase. For instance, the breaking C−H bond lengths are 1.556 (C), 1.694 (Si), 1.811 (Ge), 1.904 (Sn), and 2.078 Å (Pb), respectively, whereas the forming E−C bond lengths are 0.805 (C), 0.419 (Si), 0.377 (Ge), 0.332 (Sn), and 0.291 Å (Pb) longer than that in the $HC(CMeNPh)_2E(H)(CH_3)^+$ insertion product. These values suggest that the C−H bond insertion takes place earlier along the reaction coordinate for cations with lighter carbenic centers. Thus, the E−H and E−C bond lengths in the transition structure are more product-like for E = Sn and Pb, and more reactant-like for E = C and Si. According to the Hammond postulate,[12] the TS-CH_4−Sn and TS-CH_4−Pb should have the highest and TS-CH_4−C and TS-CH_4−Si the smallest activation barriers. This was fully confirmed by our theoretical calculations. As shown in Table 2, the barrier height (CCSD) for the C−H insertion reaction increases in the order (kcal/mol): TS-CH_4−C (+60) < TS-CH_4−Si (+69) < TS-CH_4−Ge (+87) < TS-CH_4−Sn (+103) < TS-CH_4−Pb (+128). In other words, the heavier the atomic number of the E center, the greater the C−H insertion barrier.

On the other hand, the optimized product structures (Pro-CH_4−C, Pro-CH_4−Si, Pro-CH_4−Ge, Pro-CH_4−Sn, and Pro-CH_4−Pb) are collected in Figure 2, and the calculated reaction enthalpies for insertion are given in Table 2. Again, as Figure 2 shows, the order of the E−C bond length follows the same trend as the atomic weight of the central atom E: Pro-CH_4−C (1.53 Å) < Pro-CH_4−Si (1.87 Å) < Pro-CH_4−Ge (1.94 Å) < Pro-CH_4−Sn (2.11 Å) < Pro-CH_4−Pb (2.17 Å). To our knowledge, experimental structures for such compounds are not yet known.[3] As mentioned above, a group 14 cationic carbene with a less massive but more electronegative central atom reaches the transition state relatively early, whereas one with a more massive and less electronegative central atom arrives relatively late. The former is therefore predicted to undergo a more exothermic insertion, which is borne out by our B3LYP and CCSD calculations. For example, the order of exothermicity follows the same trend as the activation energy (CCSD, kcal/mol): Pro-CH_4−C (−39) < Pro-CH_4−Si (−35) < Pro-CH_4−Ge (−7.8) < Pro-CH_4−Sn (+12) < Pro-CH_4−Pb (+47). Note that the energies of Pro-CH_4−Sn and Pro-CH_4−Pb are above those of their corresponding starting materials. This strongly implies that CH_4 insertion by $[HC(CMeNPh)_2Sn:]^+$ and $[HC(CMeNPh)_2Pb:]^+$ are energetically unfavorable and would be endothermic. Namely, our theoretical findings suggest that the insertion products of tin, and lead cationic carbenes should not be produced from the C−H bond insertion reaction of $[HC(CMeNPh)_2Sn:]^+ + CH_4 \rightarrow HC(CMeNPh)_2Sn(H)(CH_3)^+$ and $[HC(CMeNPh)_2Pb:]^+ + CH_4 \rightarrow HC(CMeNPh)_2Pb(H)(CH_3)^+$, respectively, but possibly exist if these two final products are produced via other reaction paths.

All the above DFT results can be rationalized on the basis of a configuration mixing (CM) model attributed to the work of Pross and Shaik.[13,14] According to this model, the stabilization of an insertion transition state depends on the singlet−triplet splitting ΔE_{st} ($= E_{triplet} - E_{singlet}$) of the reactant group 14 cationic carbene; that is, a smaller ΔE_{st} results in a greater transition state stabilization, a lower activation energy, a faster insertion reaction, and a greater exothermicity. Before further discussion, let us emphasize here the importance of the status of the triplet states of the group 14 cationic carbene reactants. Because two new covalent bonds have to be formed in the insertion product $HC(CMeNPh)_2E(H)(CH_3)^+$, that is, the E−H and E−C bonds (Figure 2), the bond-prepared $[HC(CMeNPh)_2E:]^+$ state thus has to have at least two open shells, and the lowest state of this type is the triplet state. Therefore, from the valence-bond point of view,[13,14] the bonding in the product can be recognized as occurring between the triplet $[HC(CMeNPh)_2E:]^+$ state and the two doublet radicals (overall singlet), the methyl radical, and the hydrogen atom. This is much the same as bonding in the water molecule, which can be considered as occurring between a triplet oxygen atom and two doublet hydrogen atoms.[15] In consequence, if a reactant $[HC(CMeNPh)_2E:]^+$ has a singlet ground-state with a small excitation energy to the triplet state, then this will bring more opportunities for the triplet state to take part in the singlet reaction and a single-step bond insertion is expected to take place more readily. As discussed earlier, our DFT results suggest an increasing trend in ΔE_{st} for the $[HC(CMeNPh)_2E:]^+$ reactant (CCSD calculations) as follows: C (46 kcal/mol) < Si (60 kcal/mol) < Ge (70 kcal/mol) < Sn (103 kcal/mol) < Pb (128 kcal/mol). This result is in accordance with the trend in activation energy and reaction enthalpy ($\Delta E^{\ddagger}$, ΔH) for group 14 cationic carbene species as discussed above. These results strongly support the predictions as mentioned previously: the smaller the ΔE_{st} of the group 14 cationic carbene, $[HC(CMeNPh)_2E:]^+$, the lower the barrier height and, in turn, the faster the insertion reaction and the greater the exothermicity.

3. Geometries and Energetics of $[HC(CMeNPh)_2E:]^+ + C_2H_4$. We next consider addition reactions that proceed via eq 2. For consistency with our previous work, the following reaction mechanism has been used to explore the cycloaddition reaction of group 14 cationic carbene systems with ethylene: reactants (Rea-C_2H_4) → transition state (TS-C_2H_4) → addition product (Pro-C_2H_4). For the systems E = C, Si, Ge, Sn, and Pb, their geometries and energetics have been calculated using the B3LYP/LANL2DZ level of theory. Selected geometrical parameters and relative energies of stationary points for the above mechanism are collected in Figure 3 and Table 3. Cartesian coordinates calculated for the stationary points at the B3LYP level are available as Supporting Information. The major conclusions drawn from the current study can be summarized as follows.

As predicted before, a cationic six-membered $[HC(CMeNPh)_2E:]^+$ species and ethylene should undergo a [1 + 2] cycloaddition with a barrier to form a cycloaddition product.

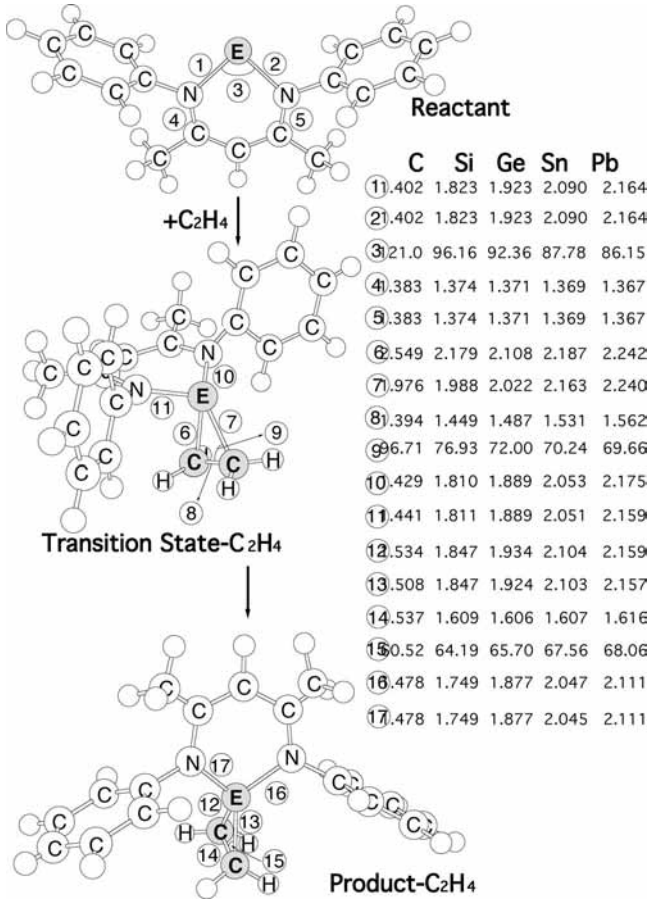

Figure 3. B3LYP/LANL2DZ optimized geometries (in Ångströms and degrees) of the reactants (singlet), transition states, and addition products of $[HC(CMeNPh)_2E:]^+$ (E = C, Si, Ge, Sn, and Pb) and C_2H_4. See Table 3 for the relative energies for each species. Hydrogens are omitted for clarity.

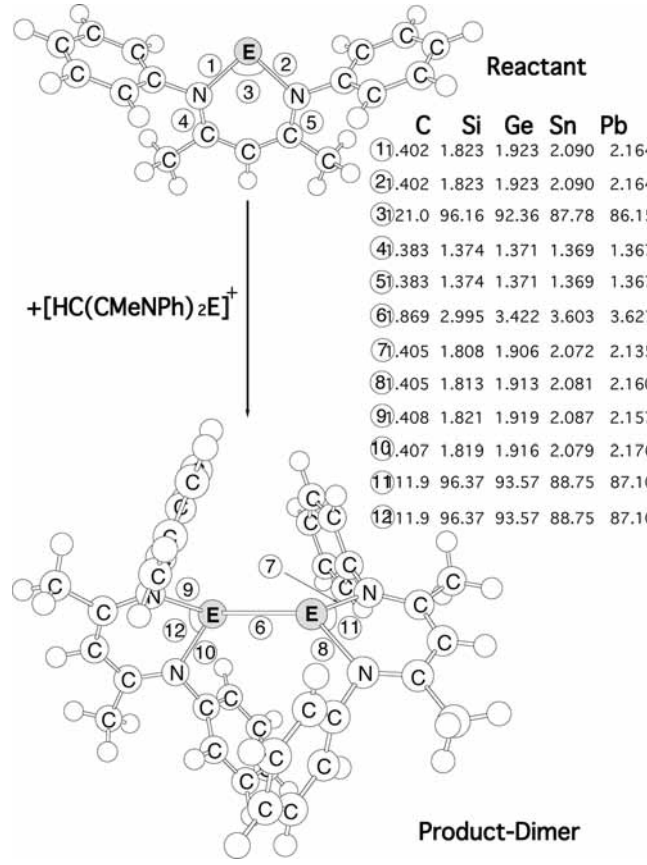

Figure 4. B3LYP/LANL2DZ optimized geometries (in Ångströms and degrees) of the reactants (singlet) and dimer products of $[HC(CMeNPh)_2E:]^+$ (E = C, Si, Ge, Sn, and Pb). For the relative energies for each species, see Table 4. Hydrogens are omitted for clarity. For more information see the text.

TABLE 3: Relative Energies for Singlet and Triplet Group 14 Cationic Carbene Species ($[HC(CMeNPh)_2E:]^+$) and for the C_2H_4 Addition Process: Reactants ($[HC(CMeNPh)_2E:]^+ + C_2H_4$) → Transition State → Addition Product[a]

system	ΔE_{st}[b] (kcal mol^{-1})	$\Delta E^{\ddagger}$[c] (kcal mol^{-1})	ΔH[d] (kcal mol^{-1})
E = C	46.19 (46.23)	32.33 (20.11)	−10.11 (−19.32)
E = Si	59.97 (60.39)	36.56 (39.29)	9.172 (−7.062)
E = Ge	67.28 (70.27)	44.39 (46.54)	34.07 (19.19)
E = Sn	71.93 (75.77)	54.35 (58.29)	50.33 (44.88)
E = Pb	77.75 (79.96)	84.57 (87.16)	81.53 (82.52)

[a] All were calculated at the B3LYP/LANL2DZ (CCSD results in parentheses) level of theory. For the B3LYP optimized structures of the stationary points, see Figure 3. [b] Energy relative to the corresponding singlet state. A positive value means the singlet is the ground-state. [c] The activation energy of the transition state, relative to the corresponding reactants. [d] The reaction enthalpy of the product, relative to the corresponding reactants.

As one can see in Table 3, it is evident that these transition states (i.e., TS-C_2H_4−C, TS-C_2H_4−Si, TS-C_2H_4−Ge, TS-C_2H_4−Sn, and TS-C_2H_4−Pb), which all are at first-order saddle points as determined by the frequency calculations at the B3LYP/LANL2DZ level, proceed in a three-center pattern involving the group 14 and two carbon atoms. Our B3LYP/LANL2DZ frequency calculations for the transition states TS-C_2H_4−C, TS-C_2H_4−Si, TS-C_2H_4−Ge, TS-C_2H_4−Sn, and TS-C_2H_4−Pb indicate that the single imaginary frequency values are 383*i*, 362*i*, 258*i*, 143*i*, and 142*i* cm^{-1}, respectively. The normal modes associated with the single imaginary frequency are consistent with the C═C activation process, primarily the C═C bond stretching with a group 14 atom migrating to the double bond. It should be pointed out that such characteristic three-centered cyclic transition states are quite analogous to mechanisms observed for the addition reactions of singlet carbene.[16,17]

Moreover, our B3LYP/LANL2DZ results demonstrate that the larger the ∠NEN bond angle, the more reactant-like the transition state structure. From Table 3, it is apparent that the length of the C═C bond for TS-C_2H_4−C, TS-C_2H_4−Si, TS-C_2H_4−Ge, TS-C_2H_4−Sn, and TS-C_2H_4−Pb is 1.394, 1.449, 1.487, 1.531, and 1.562 Å, respectively, in comparison with free ethene (1.330 Å). Besides these, one may easily see that the activation energy (kcal/mol) of the transition state follows the same trend as the singlet−triplet splitting in the cationic six-membered $[HC(CMeNPh)_2E:]^+$ system, that is, TS-C_2H_4−C (20.1) < TS-C_2H_4−Si (39.3) < TS-C_2H_4−Ge (46.5) < TS-C_2H_4−Sn (58.3) < TS-C_2H_4−Pb (87.2). That is to say, according to the CM model,[13,14] one predicts that a cationic six-membered $[HC(CMeNPh)_2E:]^+$ species with a more electronegative atom would have a larger ∠NEN bond angle, a smaller ΔE_{st} value, and a more facile cycloaddition to ethylene.

Finally, as one can see in Table 3, the energy of the final cycloproducts relative to their corresponding reactants are −19.3 (Pro-C_2H_4−C), −7.06 (Pro-C_2H_4−Si), +19.2 (Pro-C_2H_4−Ge), +44.9 (Pro-C_2H_4−Sn), and +82.5 kcal/mol (Pro-C_2H_4−Pb), indicating that reactions of cationic six-membered $[HC(CMeNPh)_2E:]^+$ molecules with more electropositive group 14 atoms (E)

TABLE 4: Relative Energies for Singlet and Triplet Group 14 Cationic Carbene Species ([HC(CMeNPh)$_2$E:]$^+$) and for the Dimerization Process: Reactants (2[HC(CMeNPh)$_2$E:]$^+$) → Dimerization Product[a]

system	ΔE_{st}[b] (kcal mol^{-1})	ΔH[c] (kcal mol^{-1})	ΔG[d] (kcal mol^{-1})
E = C	46.19	44.58	42.56
E = Si	59.97	46.41	58.39
E = Ge	67.28	54.35	60.88
E = Sn	71.93	55.82	64.71
E = Pb	77.75	58.60	68.18

[a] All were calculated at the B3LYP/LANL2DZ level of theory. For the B3LYP optimized structures of the stationary points see Figure 4. [b] Energy relative to the corresponding singlet state. A positive value means the singlet is the ground-state. [c] The reaction enthalpy of the product, relative to the corresponding reactants. [d] The Gibbs free energy (298 K) of the product, relative to the corresponding reactants.

are highly endothermic. Also, it should be noted that the order of the reaction enthalpy follows the same trend as the ∠NEN bond angle as well as the singlet−triplet splitting (ΔE_{st}). In other words, our model calculations demonstrate that the values of ΔE_{st} are remarkably diagnostic of the reactivities of cationic six-membered [HC(CMeNPh)$_2$E:]$^+$ species.

4. Geometries and Electronic Structures of Dimerization Reactions. To understand more about the kinetic stability of the cationic six-membered [HC(CMeNPh)$_2$E:]$^+$ molecule, its dimerization reaction was also investigated in this work. Selected geometrical parameters for the stationary point structures along the pathway given in eq 3 and calculated at the B3LYP/LANL2DZ level are shown in Figure 4. The relative energies obtained at the same level of theory are collected in Table 4. Cartesian coordinates for these stationary points are included in the Supporting Information. There are several important conclusions from these results to which attention should be drawn.

As expected, a double-bond between the two group 14 atoms should be formed during the dimerization reaction of two [HC(CMeNPh)$_2$E:]$^+$ molecules. Nevertheless, repeated attempts to find the transition state for a concerted dimerization of two [HC(CMeNPh)$_2$E:]$^+$ species using the DFT methodology failed. It was therefore concluded that no transition states exist on the B3LYP surface for such dimerization reactions. Furthermore, our thermodynamic results prove that all five dimers (i.e., Pro-dimer-C, Pro-dimer-Si, Pro-dimer-Ge, Pro-dimer-Sn, and Pro-dimer-Pb) contain no imaginary frequency and, in turn, can be considered as true minima on the B3LYP potential energy surfaces. As already shown in Figure 4, it is clear that the two monomer molecules are positioned with the two six-membered ring planes nearly orthogonal to each other, due to the presence of two bulky protecting groups around the group 14 center. Unfortunately, as we have mentioned earlier, because of a lack of experimental and theoretical data on such species, the geometrical values presented in this work should be considered as predictions for future investigations.

Moreover, our B3LYP computations indicate that the greater the atomic number of the group 14 element, the longer the E═E bond distance. As demonstrated in Figure 4, the trend in E═E bond length in the dimer molecule was calculated to be in the order 1.869 (C═C) < 2.995 (Si═Si) < 3.422 (Ge═Ge) < 3.603 (Sn═Sn) < 3.627 Å (Pb═Pb), correlating with the atomic size of the main group 14 element E as it changes from C to Pb. Besides this, the B3LYP calculations show that the energy of the final products (dimers) relative to their corresponding

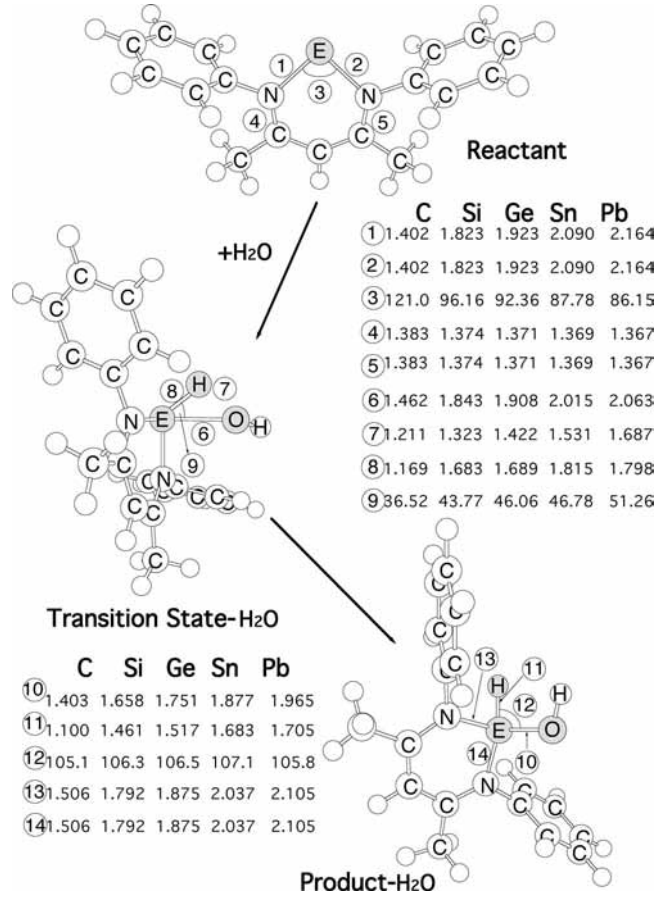

Figure 5. B3LYP/LANL2DZ optimized geometries (in Ångströms and degrees) of the reactants (singlet), transition states, and O−H insertion products of [HC(CMeNPh)$_2$E:]$^+$ (E = C, Si, Ge, Sn, and Pb) and H_2O. See Table 5 for the relative energies of each species. Hydrogens are omitted for clarity.

reactants are 44.6 (C═C), 46.4 (Si═Si), 54.4 (Ge═Ge), 55.8 (In═In), and 58.6 (Pb═Pb) kcal/mol at the CCSD level of theory. Also, we have calculated the free energy differences (ΔG) for eq 3 at 298 K, which are also given in Table 4. As shown there, the values of ΔG between reactants and dimer are 42.6, 58.4, 60.9, 64.7, and 68.2 kcal/mol for carbon, silicon, germanium, tin, and lead species, respectively. Consequently, our computational results predict that the dimerization reaction should not occur during the formation of the cationic six-membered [HC(CMeNPh)$_2$E:]$^+$ (E = C, Si, Ge, Sn, and Pb) species at room temperature.

IV. Extension

After submitting this paper, one referee suggested to calculate three kinds of chemical reactions. That is, reactants (Rea-H_2O) → transition state (TS-H_2O) → products (Pro-H_2O), reactants (Rea-HCCH) → transition state (TS-HCCH-1) → insertion product (Pro-HCCH-1), and reactants (Rea-HCCH) → transition state (TS-HCCH-2) → addition product (Pro-HCCH-2). See eqs 5–7, respectively. The optimized geometries calculated at the B3LYP/LANL2DZ level of theory involving reactants, transition states, and products are collected in Figures 5–7, respectively. The corresponding relative energies at the B3LYP level of theory are given in Tables 5 and 6, respectively. Cartesian coordinates calculated for the stationary points at the B3LYP level are available as Supporting Information.

Again, the results given in Tables 5–7 support the prediction as stated earlier, the smaller the ΔE_{st} of the group 14 cationic

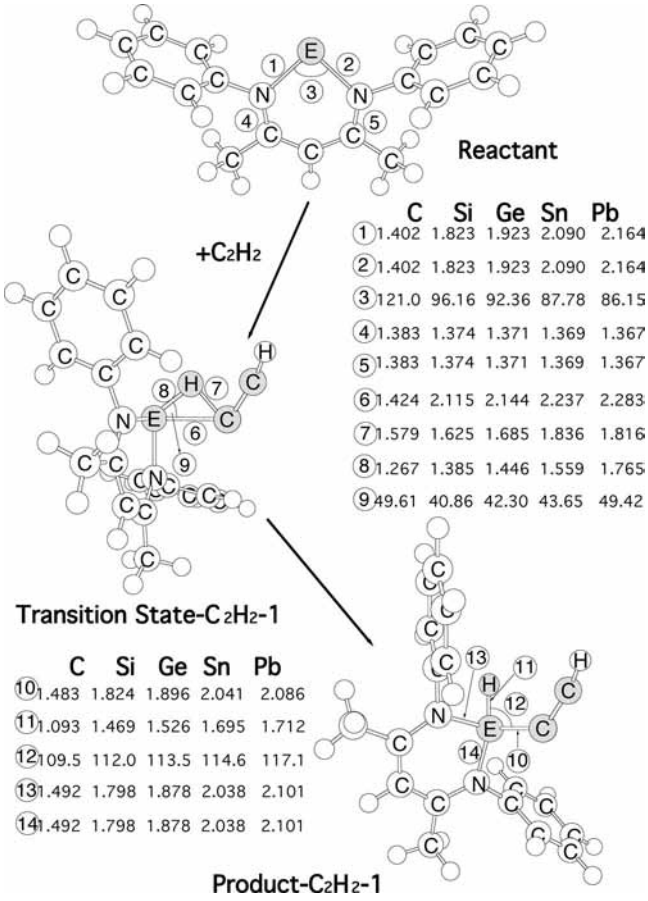

Figure 6. B3LYP/LANL2DZ optimized geometries (in Ångströms and degrees) of the reactants (singlet), transition states, and C−H insertion products of $[HC(CMeNPh)_2E:]^+$ (E = C, Si, Ge, Sn, and Pb) and C_2H_2. See Table 6 for the relative energies of each species. Hydrogens are omitted for clarity.

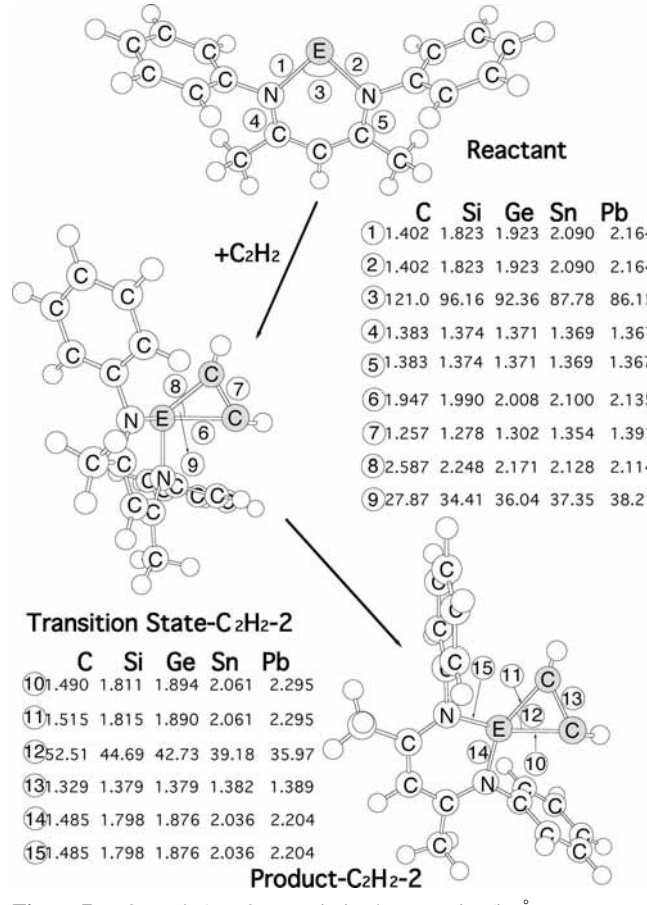

Figure 7. B3LYP/LANL2DZ optimized geometries (in Ångströms and degrees) of the reactants (singlet), transition states, and [1 + 2] cycloaddition products of $[HC(CMeNPh)_2E:]^+$ (E = C, Si, Ge, Sn, and Pb) and C_2H_2. See Table 7 for the relative energies for each species. Hydrogens are omitted for clarity.

carbene, $[HC(CMeNPh)_2E:]^+$, the lower the barrier height and, in turn, the faster the insertion reaction and the greater the exothermicity. For instance, at the B3LYP level of theory the barrier height for H_2O activation increases in the order: TS-H_2O−C (7.78 kcal/mol) < TS-H_2O−Si (20.6 kcal/mol) < TS-H_2O−Ge (31.5 kcal/mol) < TS-H_2O−Sn (34.7 kcal/mol) < TS-H_2O−Pb (56.7 kcal/mol); and for HCCH activation: TS-HCCH−C (44.7 kcal/mol) < TS-HCCH−Si (47.1 kcal/mol) < TS-HCCH−Ge (58.1 kcal/mol) < TS-HCCH−Sn (62.4 kcal/mol) < TS-HCCH−Pb (81.8 kcal/mol). Likewise, the reaction enthalpy for insertion reaction increase in the order: Pro-H_2O−C (−39.7 kcal/mol) < Pro-H_2O−Si (−35.7 kcal/mol) < Pro-H_2O−Ge (−16.1 kcal/mol) < Pro-H_2O−Sn (−4.78 kcal/mol) < Pro-H_2O−Pb (+32.5 kcal/mol) and Pro-HCCH−C (−43.8 kcal/mol) < Pro-HCCH−Si (−25.4 kcal/mol) < Pro-HCCH−Ge (−6.78 kcal/mol) < Pro-HCCH−Sn (+6.61 kcal/mol) < Pro-HCCH−Pb (+38.8 kcal/mol). Similarly, after considering the thermodynamic factors, Tables 5–7 also show that the Gibbs free energies give the same trend as predicted earlier. Note that the Gibbs free energetics of [1 + 2] cycloaddition products (Pro-HCCH-2) are all above those of their corresponding reactants. This indicates that the acetylene [1 + 2] cycloaddition reactions by cyclic $[HC(CMeNPh)_2E:]^+$ molecules are energetically unfavorable and would be endothermic. On the other hand, the Gibbs free energetics of C−H insertion products (Pro-HCCH-1) are only two cases below than those of the corresponding reactants. Namely, our theoretical findings demonstrate that the C−H bond activation reactions by cyclic $[HC(CMeNPh)_2C:]^+$ and $[HC(CMeNPh)_2Si:]^+$ are energetically favorable and can obtain their insertion products at room temperature. In consequence, $[HC(CMeNPh)_2C:]^+$ and $[HC(CMeNPh)_2Si:]^+$ with

TABLE 5: Relative Energies for Singlet and Triplet Group 14 Cationic Carbene Species ($[HC(CMeNPh)_2E:]^+$) and for the H_2O Insertion Process: Reactants ($[HC(CMeNPh)_2E:]^+ + C_2H_4$) → Transition State → Insertion Product[a]

system	ΔE_{st}[b] (kcal mol^{-1})	$\Delta E^{\ddagger}$[c] (kcal mol^{-1})	ΔH[d] (kcal mol^{-1})
E = C	46.19	7.775 [17.93]	−39.74 [−23.77]
E = Si	59.97	20.62 [30.32]	−35.66 [−29.90]
E = Ge	67.28	31.51 [41.92]	−16.14 [−4.456]
E = Sn	71.93	34.70 [45.94]	−4.784 [6.723]
E = Pb	77.75	56.74 [66.08]	32.52 [42.56]

[a] All were calculated at the B3LYP/LANL2DZ level of theory. For the B3LYP optimized structures of the stationary points, see Figure 5. The Gibbs free energies are given in the square bracket. [b] Energy relative to the corresponding singlet state. A positive value means the singlet is the ground-state. [c] The activation energy of the transition state, relative to the corresponding reactants. [d] The reaction enthalpy of the product, relative to the corresponding reactants.

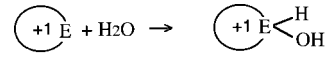

(5)

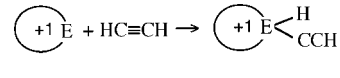

(6)

TABLE 6: Relative Energies for Singlet and Triplet Group 14 Cationic Carbene Species ($[HC(CMeNPh)_2E:]^+$) and for the C_2H_2 Insertion Process: Reactants ($[HC(CMeNPh)_2E:]^+ + C_2H_4$) → Transition State → Insertion Product([a])

system	ΔE_{st}[b] (kcal mol^{-1})	$\Delta E^{\ddagger}$[c] (kcal mol^{-1})	ΔH[d] (kcal mol^{-1})
E = C	46.19	44.67 [34.84]	−43.81 [−34.27]
E = Si	59.97	47.08 [56.05]	−25.40 [−16.13]
E = Ge	67.28	58.09 [68.43]	−6.778 [4.497]
E = Sn	71.93	62.39 [72.75]	6.608 [17.21]
E = Pb	77.75	81.84 [90.86]	38.81 [48.15]

[a] All were calculated at the B3LYP/LANL2DZ level of theory. For the B3LYP optimized structures of the stationary points, see Figure 6. The Gibbs free energies are given in the square bracket. [b] Energy relative to the corresponding singlet state. A positive value means the singlet is the ground-state. [c] The activation energy of the transition state, relative to the corresponding reactants. [d] The reaction enthalpy of the product, relative to the corresponding reactants.

TABLE 7: Relative Energies for Singlet and Triplet Group 14 Cationic Carbene Species ($[HC(CMeNPh)_2E:]^+$) and for the C_2H_2 Addition Process: Reactants ($[HC(CMeNPh)_2E:]^+ + C_2H_4$) → Transition State → Insertion Product[a]

system	ΔE_{st}[b] (kcal mol^{-1})	$\Delta E^{\ddagger}$[c] (kcal mol^{-1})	ΔH[d] (kcal mol^{-1})
E = C	46.19	44.67 [21.20]	−43.81 [11.71]
E = Si	59.97	47.08 [24.16]	−25.40 [29.16]
E = Ge	67.28	58.09 [36.87]	−6.778 [56.48]
E = Sn	71.93	62.39 [80.21]	6.608 [73.20]
E = Pb	77.75	81.84 [83.38]	38.81 [104.7]

[a] All were calculated at the B3LYP/LANL2DZ level of theory. For the B3LYP optimized structures of the stationary points, see Figure 7. The Gibbs free energies are given in the square bracket. [b] Energy relative to the corresponding singlet state. A positive value means the singlet is the ground-state. [c] The activation energy of the transition state, relative to the corresponding reactants. [d] The reaction enthalpy of the product, relative to the corresponding reactants.

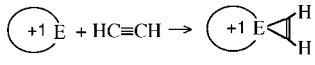

(7)

((+1 E = HC(CMeNPh) 2E ; E = C, Si, Ge Sn, and Pb)

acetylene would prefer to undergo the C−H bond insertion reaction, rather than the [1 + 2] cycloaddition reaction. These computational results are in good agreement with the available experimental observations.c,d

V. Conclusion

In this work, we have studied the mechanisms of four kinds of chemical reactions of cationic six-membered $[HC(CMeNPh)_2E:]^+$ species using density functional theory and CCSD methods. It should be pointed out that this study has provided the first theoretical demonstration of the reaction trajectory and theoretical estimation of the activation energy and reaction enthalpy for these chemical processes.

Our present theoretical investigations demonstrate that the chemical reactivity of carbon, silicon, germanium, tin, and lead species decrease in the order C > Si > Ge > Sn > Pb. From another point of view, our theoretical findings confirm a general belief that one of the important influences on the isolability of a group 14 cationic carbene species is its group 14 atom center.[3] That is to say, our theoretical works strongly imply that the cationic six-membered group 14 carbene species (E = C, Si, Ge, Sn, and Pb) should be stable, and can be readily synthesized and isolated at room temperature.

Regardless of the chemical reaction considered, it is found that a knowledge of the singlet−triplet splitting of the cationic six-membered $[HC(CMeNPh)_2E:]^+$ molecule is of great importance in understanding its reactivity because it can affect the driving force for the chemical reaction. Qualitatively, the greater the ∠NEN bond angle and the smaller the ΔE_{st} of the cationic six-membered $[HC(CMeNPh)_2E:]^+$ molecule, the lower its activation barrier and, in turn, the more rapid its chemical reactions are. Specifically, electronic as well as steric factors should play an important role in determining the chemical reactivity of the cationic six-membered group 14 carbeneoids from both kinetic and thermodynamic viewpoints.

Furthermore, we have demonstrated that the computational results can be rationalized using a simple CM model. Although the relative reactivity of various chemical species is determined by the entire potential energy surface, the concepts of the CM model, focusing on the singlet−triplet splitting in the reactants, allows one to assess quickly the relative reactivity of a variety of cationic six-membered group 14 carbene species without specific knowledge of the actual energies of the interactions involved. In spite of its simplicity, our approach can provide chemists with important insights into the factors controlling these chemical reactions, and thus permit them to predict the reactivity of some unknown cationic six-membered group 14 carbene species. The predictions may be useful as a guide to future synthetic efforts and to indicate problems that merit further study by both theory and experiment. This should be helpful for further developments in group 14 heavy-carbene chemistry.

We encourage experimentalists to carry out further experiments to confirm our predictions.

Acknowledgment. The authors are grateful to the National Center for High-Performance Computing of Taiwan for generous amounts of computing time. They also thank the National Science Council of Taiwan for the financial support. Special thanks are also due to Referees one and two for very helpful suggestions and comments.

Supporting Information Available: B3LYP/LANL2DZ optimized geometries and B3LYP energies. This material is available free of charge via the Internet athttp://pubs.acs.org.

References and Notes

(1) For recent reviews, see: (a) Barrau, J.; Escudié, J.; Satgé, J. *Chem. Rev.* **1990**, *90*, 283. (b) Weidenbruch, M. *Eur. J. Inorg. Chem.* **1999**, 373. (c) 1c. (d) Kühl, O. *Coord. Chem. Rev.* **2004**, *248*, 411.

(2) (a) Arduengo III, A. J.; Harlow, R. L.; Kline, M. *J. Am. Chem. Soc.* **1991**, *113*, 361. (b) Arduengo III, A. J.; Dias, H. V. R.; Harlow, R. L.; Kline, M. *J. Am. Chem. Soc.* **1992**, *114*, 5530. (c) Arduengo III, A. J.; Goerlich, J. R.; Marshall, W. J. *J. Am. Chem. Soc.* **1995**, *117*, 11027. (d) Alder, R. W.; Allen, P. R.; Murray, M.; Orpen, A. G. *Angew. Chem., Int. Ed. Engl.* **1996**, *35*, 1121. (e) Arduengo III, A. J.; Goerlich, J. R.; Marshall, W. J. *Liebigs Ann. Recl.* **1997**, 365. (f) Alder, R. W.; Butts, C. P.; Orpen, A. G. *J. Am. Chem. Soc.* **1998**, *120*, 11526. (g) Liu, Y.; Lindner, P. E.; Lemal, D. M. *J. Am. Chem. Soc.* **1999**, *121*, 10626. (h) Hahn, F. H.; Wittenbecher, L.; Le Van, D.; Fröhlich, R. *Angew. Chem., Int. Ed.* **2000**, *39*, 541. (i) Heinemann, C.; Müller, T.; Apeloig, Y.; Schwarz, H. *J. Am. Chem. Soc.* **1996**, *118*, 2023. (j) Boehme, C.; Frenking, G. *J. Am. Chem. Soc.* **1996**, *118*, 2039. (k) Alder, R. W.; Blake, M. E.; Bortolotti, C.; Bufali, S.; Butts, C. P.; Linehan, E.; Oliva, J. M.; Orpen, A. G.; Quayle, M. J. *Chem. Commun.* **1999**, 241. (l) Guillen, F.; Winn, C. L.; Alexakis, A. *Tetrahedron: Asymmetry* **2001**, *12*, 2083.

(3) (a) Driess, M.; Yao, S.; Brym, M.; Wüllen, C. V. *Angew. Chem., Int. Ed.* **2006**, *45*, 4349. (b) Driess, M.; Yao, S.; Brym, M.; Wüllen, C. V. *Angew. Chem., Int. Ed.* **2006**, *45*, 6730. (c) Yao, S.; Brym, M.; Wullen, C. van.; Driess, M. *Angew. Chem., Int. Ed.* **2007**, *46*, 4159. (d) Yao, S.; Wullen, C. van.; Sun, X.-Y.; Driess, M. *Angew. Chem., Int. Ed.* **2008**, *47*, 3250.

(4) (a) Ding, M.; Ma, Q.; Roesky, H. W.; Herbst-Irmer, R.; Usóm, I.; Noltemeyer, M.; Schmidt, H.-G. *Organometallics* **2002**, *21*, 5216. (b) Driess, M.; Yao, S.; Brym, M.; Wüllen, C. V.; Lentz, D. *J. Am. Chem. Soc.* **2006**, *128*, 9628. (c) Xiong, Y.; Yao, S.; Brym, M.; Driess, M. *Angew. Chem., Int. Ed.* **2007**, *46*, 4511.

(5) (a) Becke, A. D. *Phys. Rev. A* **1988**, *38*, 3098. (b) Becke, A. D. *J. Chem. Phys.* **1993**, *98*, 5648.

(6) Lee, C.; Yang, W.; Parr, R. G. *Phys. Rev. B,* **1988**, *37*, 785.

(7) (a) Dunning, T. H., Jr.; Hay, P. J. In *Modern Theoretical Chemistry*, Schaefer, H. F., III, Ed.; Plenum: New York, 1976; p1−28. (b) Hay, P. J.; Wadt, W. R. *J. Chem. Phys.* **1985**, *82*, 270. (c) ibid., 1985, *82*, 284. (d) ibid., 1985, *82*, 299.

(8) Pople, J. A.; Head-Gordon, M.; Raghavachari, K. *J. Chem. Phys.* **1987**, *87*, 5968.

(9) Frisch, M. J.; Trucks, G. W.; Schlegel, H. B.; Scuseria, G. E.; Robb, M. A.; Cheeseman, J. R.; Zakrzewski, V. G.; Montgomery, Jr., J. A.; Stratmann, R. E. ; Burant, J. C.; Dapprich, S.; Millam, J. M.; Daniels, A. D.; Kudin, K. N.; Strain, M. C.; Farkas, O.; Tomasi, J.; Barone, V.; Cossi, M.; Cammi, R.; Mennucci, B.; Pomelli, C.; Adamo, C.; Clifford, S.; Ochterski, J.; Petersson, G. A.; Ayala, P. Y.; Cui, Q.; Morokuma, K.; Malick, D. K. ; Rabuck, A. D.; Raghavachari, K.; Foresman, J. B.; Cioslowski, J.; Ortiz, J. V.; Baboul, A. G.; Stefanov, B. B. ; Liu, Liashenko, G. ; Piskorz, A.; Komaromi, P.; I.; Gomperts, R.; Martin, R. L.; Fox, D. J.; Keith, T.; Al-Laham, M. A.; Peng, C. Y.; Nanayakkara, A.; Gonzalez, C.; Challacombe, M.; Gill, P. M. W.; Johnson, B.; Chen, W.; Wong, M. W.; Andres, J. L.; Gonzalez, C.; Head-Gordon, M.; Replogle, E. S. and Pople, J. A. Gaussian, Inc., Pittsburgh PA, 2003.

(10) (a) Pyykkö, P.; Desclaux, J.-P. *Acc. Chem. Res.* **1979**, *12*, 276. (b) Kutzelnigg, W. *Angew. Chem., Int. Ed. Engl.* **1984**, *23*, 272. (c) Pyykkö, P. *Chem. Rev.* **1988**, *88*, 563. (d) Pyykkö, P. *Chem. Rev.* **1997**, *97*, 597.

(11) (a) Su, M.-D.; Chu, S.-Y. *Inorg. Chem.* **1999**, *38*, 4819. (b) Su, M.-D. *J. Phys. Chem. A.* **2002**, *106*, 9563.

(12) Hammond, G. S. *J. Am. Chem. Soc.* **1954**, *77*, 334.

(13) For details, see: (a) Shaik, S.; Schlegel, H. B.; Wolfe, S. In *Theoretical Aspects of Physical Organic Chemistry*, John Wiley & Sons Inc., USA, 1992. (b) Pross, A. In *Theoretical and Physical principles of Organic Reactivity*, John Wiley & Sons Inc., USA, 1995. (c) Shaik, S. *Prog. Phys. Org. Chem.* **1985**, *15*, 197.

(14) For the first paper that originated the CM model, see: (a) Shaik, S. *J. Am. Chem. Soc.* **1981**, *103*, 3692. For information about the most updated review of the CM model, one can see: (b) Shaik, S.; Shurki, A. *Angew. Chem., Int. Ed.* **1999**, *38*, 586.

(15) Su, M.-D. *Chem. Eur. J.* **2004**, *10*, 5877.

(16) (a) Hoffmann, R. *J. Am. Chem. Soc.* **1968**, *90*, 1475. (b) Zurawski, B.; Kutzelnigg, W. *J. Am. Chem. Soc.* **1978**, *100*, 2654. (c) Rondan, N. G.; Houk, K. N.; Moss, R. A. *J. Am. Chem. Soc.* **1980**, *102*, 1770.

(17) Su, M.-D. *J. Phys. Chem.* **1996**, *100*, 4339 and related references therein.

JP8026397